

## RECOMMENDED PROCEDURE FOR DETERMINATION OF RELATIVE PERMEABILITIES

Roland Lenormand and Guillaume Lenormand, Cydarex, France

*This paper was prepared for presentation at the International Symposium of the Society of Core Analysts held in Snowmass, Colorado, USA, 21-26 August 2016*

### ABSTRACT

This paper discusses the basic mechanisms involved during determination of oil/water imbibition relative permeabilities ( $K_r$ ).

One-step experiments (only one injection pressure or flow-rate) generally referred to as JBN experiments must be discarded even if experiments are interpreted with  $P_c$  curves. Their interpretation is based on transient flow dominated by viscous fingering and/or channeling, which does not represent "true" pore-scale relative permeability.

A more accurate UnSteady-State (USS) experiment requires 7 to 10 steps. After the first step, saturations become more uniform and flows are then controlled by local  $K_r$ . The range of saturation is controlled by the balance between viscous and capillary forces and works only for the negative part of the  $P_c$  curve. The experiment is difficult to design if the  $P_c$  curve is not well-known.

Simultaneous injection of oil and water (steady-state, SS) allows a more precise control of saturations. When two fluids are injected at high flow rates, saturation is close to being uniform on a large part of the plug, and its value is controlled by the ratio of viscous forces in the two fluids. This method can be used for any type of wettability.

Based on these observations, the recommended procedure is a compromise between SS and USS methods. We also show that laboratory fluid velocities are much higher than reservoir velocities and discuss how to deal with this issue.

### INTRODUCTION

The determination of relative permeabilities by displacements is still a subject of much discussion in oil companies. There is always a debate between Steady-State (SS) and UnSteady-State (USS) methods. The purpose of this paper is to explain the physical mechanisms that govern these displacements, and how they affect the determination of relative permeabilities.

For oil and water displacements, the following definitions are used, independently of wettability: **drainage** is a displacement leading to an increase of oil saturation, and **imbibition** to an increase of water saturation. We will use oil/water imbibition, the most

common case for relative permeabilities. Results can easily be extended to other types of displacements, such as gas drainage.

Kr curves are defined and calculated at local scale, the scale of a Representative Elementary Volume where the two-phase Darcy's laws are written:

$$\frac{Q_w}{A} = -\frac{K K_{rw}}{\mu_w} \frac{\partial P_w}{\partial x} ; \quad \frac{Q_o}{A} = -\frac{K K_{ro}}{\mu_o} \frac{\partial P_o}{\partial x} \quad (1)$$

where, Q is flow rate, K absolute permeability, Kr relative permeability,  $\mu$  viscosity, P pressure and x the distance along the sample from the injection face. Indices are "w" for water and "o" for oil. Capillary pressure is defined by  $P_c = P_o - P_w$ .

A laboratory experiment is not a "small scale" representation of the reservoir. Especially, the residual oil saturation (Sor) obtained in laboratory depends on laboratory conditions, sample length, flow rates, etc. and differs from the recovery at reservoir scale, controlled by other parameters (geological structure, well implementation, etc.). The purpose of a laboratory experiment is to determine a full curve of relative permeabilities (Kr) as functions of water saturation (Sw) in a very large range of saturation that covers or even exceeds the saturations encountered in the reservoir.

For a given type of displacement (drainage or imbibition), the Kr curves are assumed to be independent of fluid velocities. This means that the viscous coupling between the fluids is negligible, as if the two fluids were flowing in separate channels (see discussion by Ayub and Bentsen [1]). With this assumption, the Kr curves are the same for SS, USS and other types of displacements such as centrifuge experiments. This assumption is in contradiction with the discontinuous flows observed at high flow rates both in micromodel experiments and Digital Rock Physics simulations. It is also often observed that Pc curves determined by history matching differ from Pc curves measured by porous plate or centrifuge methods. Lackner *et al.* [2] attribute this difference to "dynamic capillary pressures" and recommend local pressure measurements using semi-permeable membranes. We will not discuss this point here and assume that both Kr and Pc curves do not depend on fluid velocity.

We will start by discarding the JBN method, in which the information obtained is limited and not accurate, especially in terms of Sor. Then we will analyze the USS and SS methods in terms of balance between viscous forces and capillary forces. Finally we will compare laboratory experiments to numerical simulations at reservoir scale to discuss the problem of fluid velocities and the important notion of Sor.

### **ONE FLUID INJECTED –ONE STEP (JBN)**

This simple experiment of water displacing oil in a sample at irreducible saturation Swi, is usually referred to as JBN, from the name of the authors of the paper describing the Kr

analytical calculation [3]. This method is still often used, because it is quick and cheap, but it presents several drawbacks.

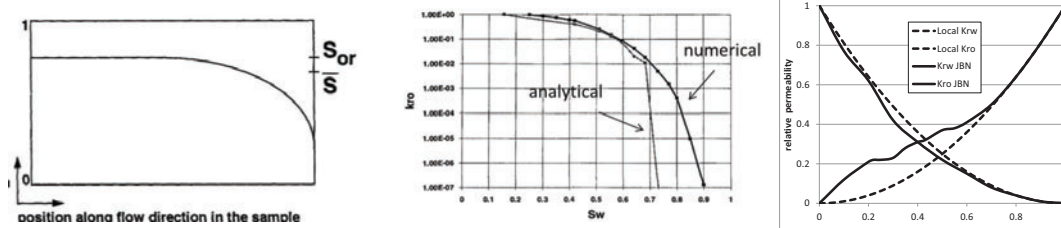


Figure 1 - (from Kokkedee *et al*)  
Saturation profile along the plug.

Figure 2 - (from Kokkedee *et al*).  
Analytical and numerical  $K_{ro}$ .

Figure 3 -  $K_r$  determination assumed on a heterogeneous sample (from Fenwick *et al.*)

More than 20 years ago, Kokkedee *et al.* [4] showed that there was always an important error on  $S_{or}$  when the JBN method was used. Whatever the reservoir type,  $S_{or}$  obtained by numerical history matching with capillary pressures is always smaller than the JBN  $S_{or}$  by 15% to 30%. The explanation is illustrated on Figure 1. The JBN calculation assumes a uniform saturation over the sample; however the profile is not uniform and drops near the outlet due to capillary effects. Although the average, derived from the effluent balance, is the same, the "local" saturation near the inlet face is larger than the average saturation. Figure 2 shows the effect on the oil  $K_r$  curve.

Another drawback is channeling. In 1988, Mohanty and Miller [5] wrote: "Results illustrate that the early part of the JBN method relative permeability is dominated by fingering and heterogeneity effects. But the later part ( $> 1PV$ ) represents the relative permeability of the end-face saturation". This result has been confirmed and illustrated by numerical simulations (Fenwick *et al.* [6]). In their study, the sample is represented as a 2-Dimensional heterogeneous permeability field with uniform Corey-shapes  $K_r$  curves for all the grids (dashed lines in Figure 3). The displacement is computed using a streamlines method and the  $K_r$  curves are determined from the production and pressure drop, as in a real experiment (solid lines). At low saturations,  $K_{rw}$  is larger than the local value because water is flowing in channels more permeable than the average. At the end of the experiment,  $K_r$  are close to the local values. The beginning of displacement is also prone to viscous fingering with an adverse mobility ratio (see for instance Sarma *et al.* [7]). Due to all these problems the one-step injection of water (JBN type experiment) is no longer recommended, even if numerical simulations are used with  $P_c$  curves. Multi-step experiments, either SS or USS, provide more accurate results.

## MULTI-STEP EXPERIMENTS

For both USS and SS multi-step experiments, the relative permeabilities are determined by history matching of the transient and stabilized parts of differential pressure and oil production. The numerical simulation takes into account a  $P_c$  curve, either measured or adjusted from the experimental results together with  $K_r$ . As for JBN, the heterogeneity plays a role at the beginning of the first displacement. At the end of the first step and all

the further steps the sample is assumed uniformly saturated with the two fluids and that the  $K_r$  are not affected by channeling and fingering.

Using numerical optimization does not provide "points"  $K_r$  values as for analytical calculations, but an analytical curve (Corey, LET, etc.) determined by minimizing the mean square root difference between experimental and calculated parameters during both transient and stabilized regimes. The most accurate determination of the  $K_r$  curves is when average saturations are numerous and regularly spaced.

### Physical mechanisms during USS multi-step displacements

In imbibition, only water is injected, starting at a low flow rate and allowing for stabilization of oil production and differential pressure. Then the water rate is increased, until stability is reached and the process is repeated for 5 to 10 steps. At each step the average saturation increases. We will show that in a USS experiment, average saturation at each step is controlled by the balance between viscous forces and capillary forces. Another important result is that the differential pressure is equal to capillary pressure at entrance when stabilization is reached.

For illustration on a general case, the  $P_c$  curve is assumed to have a positive and negative part (mixed wettability). For any step, when stabilization is reached, the water and oil pressures along the samples are schematically displayed in Figure 4a:

- At outlet, the capillary pressure is assumed to be zero; consequently both oil and water are equal to the outlet imposed pressure, taken as reference ( $P = 0$ ).
- The pressure in oil is uniform since oil is no longer flowing when equilibrium is reached (no gravity).

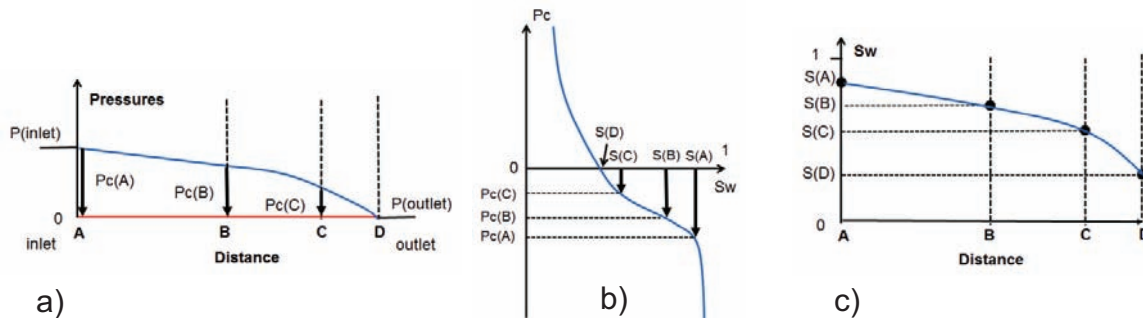


Figure 4 - USS displacement: a) pressures profiles at equilibrium (water blue, oil red), arrows represent the capillary pressure at several locations along the sample, b) determination of corresponding saturations from the  $P_c$  curve, c) saturation profile.

- Water is flowing through the sample and since the outlet pressure is 0, the pressure in water is positive everywhere along the sample (a fluid flows from higher to lower pressure). The pressure measured in the inlet end-piece is the highest pressure between the water and oil pressures inside the sample at the entrance, equal to the pressure in water (this point is discussed in [8]) Since  $P_c = P_{\text{oil}} - P_{\text{water}}$ ,  $P_c$  is negative at any location along the sample (arrows in Figure 4a). Consequently, the difference

of pressures measured between the inlet and outlet end pieces is equal to the opposite of the capillary pressure at inlet face (Figure 4a). This property is the principle of determination of the  $P_c$  curve by the semi-dynamic method [8].

- From the value of  $P_c$  at any location (B, C, D), the corresponding saturation is imposed by the capillary pressure curve (Figure 4b), leading to the saturation profile (Figure 4c).
- At outlet  $P_c=0$  and the corresponding saturation  $S(D)$  is equal to the saturation at  $P_c=0$  (where the curve cuts the saturation axis). For an "oil-wet" sample, with totally negative  $P_c$  curve, the saturation at outlet is equal to  $S_{wi}$ .

Figure 5 shows the flow rate increased by a factor 2. Most of pressures are now in the near vertical part of the  $P_c$  curve (Figure 5a and b). Saturation is more uniform on a large part of the sample with a smaller capillary end effect. Average saturation of water has increased and during the experiment a production of oil has been observed.

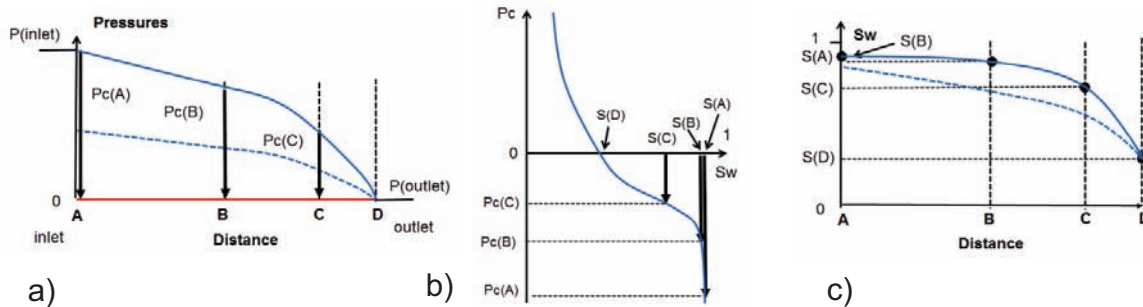


Figure 5 - USS displacement: similar to Figure 4, but with a higher flow rate a) pressure profiles in solid line, previous profiles in dashed lines, b) higher local  $P_c$  leads to higher local water saturations, c) saturation profile with the higher flow rate (solid line) showing a decrease of the extend of the capillary end effect.

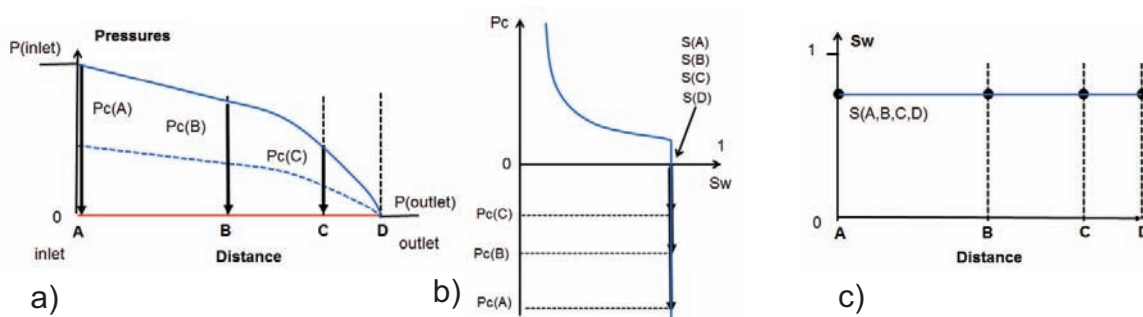


Figure 6 - Pressure and saturation profiles for a water-wet sample. Since  $P_c$  is negative, the corresponding saturation is always equal to  $1-S_{or}$ .

For a water-wet sample (Figure 6), the water pressure profile may defer from the previous case since  $K_r$  are different, but the overall shape is similar with positive pressures everywhere in water that is flowing. Capillary pressure along the sample is always negative and for all locations, the local saturation is equal to the maximum value ( $1-S_{or}$ ).

When flow rate is increased, saturations do not change since they are at their maximum values and there is no production after the first step.

The main conclusion is that capillary pressure is always negative along the sample. Consequently, local saturations are determined from the negative part of the Pc curve. In drainage it is the opposite.

**Numerical example USS**

We now illustrate the previous explanation using a numerical simulation with the commercial software CYDAR (<http://www.cydarex.fr>). Sample, fluid properties and Kr are given in Table 1 and flow rates in Table 2.

Table 1 - Sample and fluid properties for numerical simulations

type of displacement		imbibition
disposition		horizontal
length	cm	8
Diameter	cm	4
Base permeability	mD	100
porosity	frac	0.3
water viscosity	cP	1
water density	g/cm <sup>3</sup>	1
oil viscosity	cP	5
oil density	g/cm <sup>3</sup>	1
initial Sw	frac	0.2
final Sw	frac	0.8
Krw_max	frac	0.5
Kro_max	frac	0.5
Corey exponent water		3
Corey exponent oil		3

Table 2 - Flow rates during the USS experiment

duration (hour)	5	5	5	5	5	5	5
rate cc/h	2	20	100	250	450	500	1000

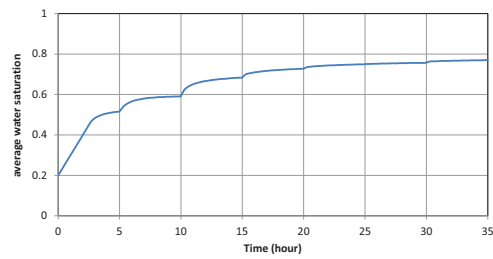


Figure 7 - USS experiment: Water average saturation.

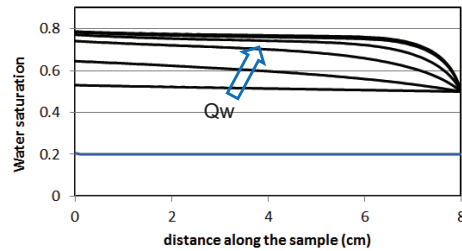


Figure 8 - USS experiment: saturation profiles

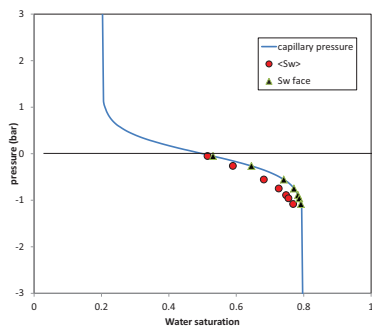


Figure 9 - USS simulation: inlet face capillary pressure versus average water saturations and inlet face saturations;

Figure 7 shows the average water saturation as function of time. Figure 8 shows saturation profiles at end of each step. For each step there is an increase of average water saturation and consequently additional production of oil.

Figure 9 shows capillary pressure at the inlet face at each stabilized step as function of the average saturation and local saturation. As explained previously, only saturations corresponding to  $P_c < 0$  are obtained.

### Physical mechanisms during SS multi-step displacements

Oil and water are injected together starting with 100 % of oil at  $S_{wi}$ . Then several flow rates (5 to 10) are used by increasing the fraction of water until 100% of water is injected. The displacement mechanisms are more complicated than for the USS case since there are now three types of forces: viscous forces in each fluid and capillary forces.

At the beginning of the experiment, the flow rate is much higher in oil than in water (low water fractional flow) and  $P_c > 0$  since pressure in oil is higher than pressure in water (Figure 10a). The local saturations correspond to the positive part of the  $P_c$  curve (Figure 10b and 10c). For higher water fractional flow,  $P_c$  is negative and local saturations correspond to the negative part of the  $P_c$  curve (Figure 11).

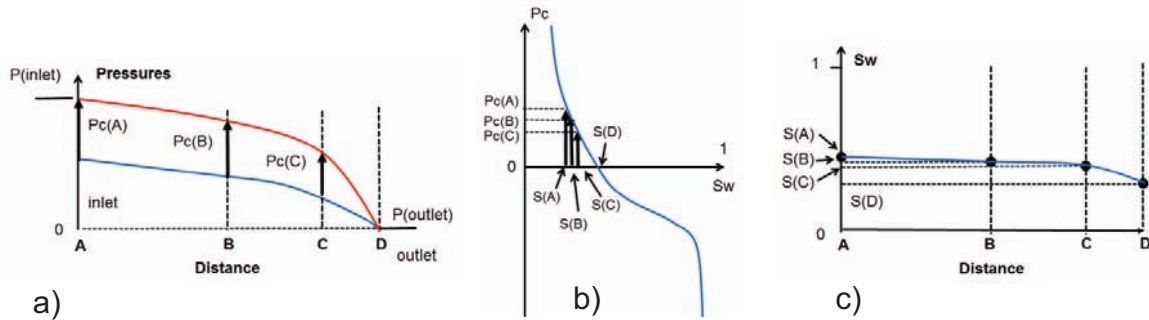


Figure 10 - SS displacement at low water fractional flow: pressure is higher in oil and capillary pressure is positive

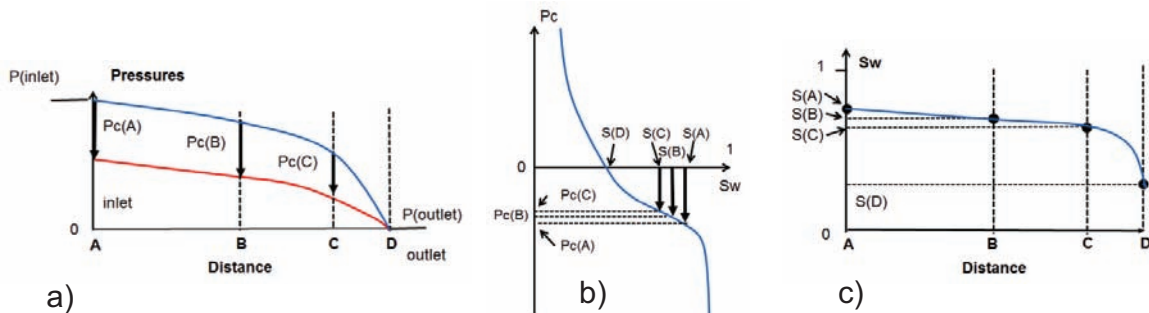


Figure 11 - SS displacement at high water fractional flow: pressure is higher in water and capillary pressure is negative

### Numerical example SS

Experiments are simulated using the same fluids and sample properties as for the USS case (Table 1) with 3 total flow rates  $Q_t = 2, 20,$  and  $1000$  cc/h. Saturation profiles at end of experiments are shown in Figure 12.

Figure 13 and Figure 14 display the fractional flow as function of average saturation. The numerical fractional flow  $Q_w/(Q_w+Q_o)$  is obtained from the simulations when stabilization is reached and the analytical values are derived from Darcy's law with the assumption of  $P_c=0$ :

$$f_w = \frac{Kr_w}{\mu_w} \bigg/ \left( \frac{Kr_w}{\mu_w} + \frac{Kro}{\mu_o} \right) \tag{2}$$

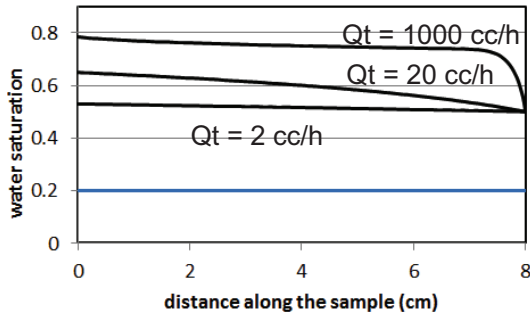


Figure 12 - saturations profiles at end of experiment for 3 total flow rates.

At high total flow rate,  $Q_t = 1000 \text{ cc/h}$  (Figure 13), analytical and numerical fractional flows are very close and well-spaced saturations can be determined over all the range of saturations by imposing the fractional flow, independently of the capillary pressure (negligible forces). For lower total flow rate, capillary forces are acting and the numerical fractional flow is no longer close to the analytical one (Figure 14).

In addition, for the lowest total flow rate case (2 cc/h), the range of saturation decreases and the main value is centered around 0.5 where  $P_c = 0$ . For  $Q_t = 20 \text{ cc/h}$ , the average saturation is only in the range 0.3 – 0.6. In the limit of very low flow rate (dashed line in Figure 14), viscous forces are negligible and the final saturation is uniform and equal to 0.5 (spontaneous imbibition).

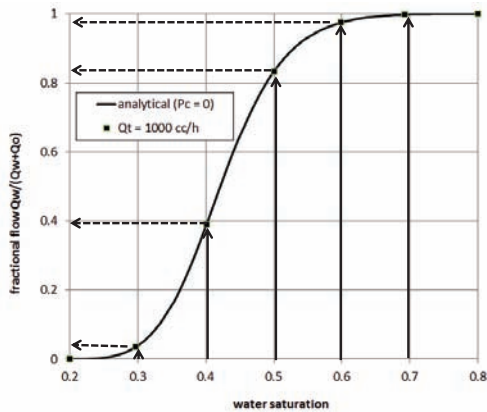


Figure 13 - High total flow rate: Analytical and numerical fractional flows are very close and well-spaced saturations can be determined by imposing the fractional flow.

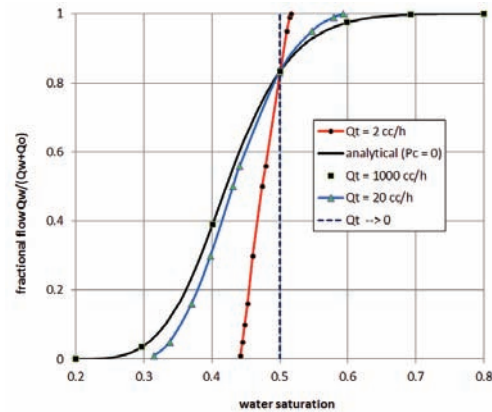


Figure 14 - Analytical and numerical fractional flows as function of average saturation for several total flow rates.

## RESERVOIR SCALE DISPLACEMENT MECHANISMS

We will present results of numerical simulation at reservoir scale to illustrate the applications and limitations of laboratory experiments. The reservoir is schematically represented by a 200 meters 1-D medium with same permeability and porosity than the laboratory sample. For Kr properties, we have used 2 cases:

- **Low mobility**, same as the laboratory simulations with Corey exponents  $\alpha = 3$ ;
- **High mobility**, same other properties but with Corey exponents  $\alpha = 2$ .

For field velocity, we have used the rule of thumb of 1 foot/day and chosen 0.7 foot/day, corresponding to the laboratory injection at 2 cc/h (Table 1). Oil production during 30 years is shown in Figure 15. As expected, production is faster for high mobility. An important result is that after 30 years, even if oil rate is very low, there is still an important pressure gradient in oil along the reservoir, close to the gradient in water and the capillary pressure is higher than -1.2 bar everywhere, even for the high mobility case (Figure 16). From  $P_c$  profiles, we have calculated saturation and corresponding Kroil profiles (Figure 17). Another important point is that Kroil is always larger than  $10^{-4}$  (dashed red line) except very close to the injection well.

Table 3 - Equivalence between laboratory total flow rate and front velocity

cc/h	2	20	100	500	1000
foot/day	0.7	6.5	65	162	323

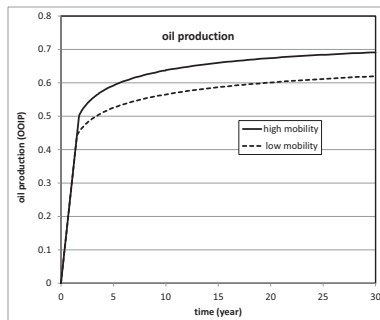


Figure 15 - Oil production during 30 years.

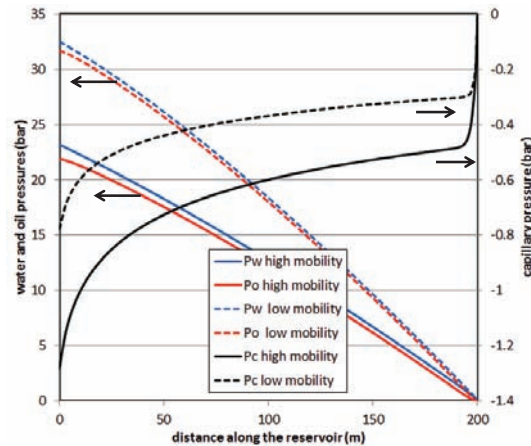


Figure 16 - Numerical simulation for a 1-D reservoir after 30 years of production: water and oil pressure profiles and capillary pressure for 2 values of oil mobility.

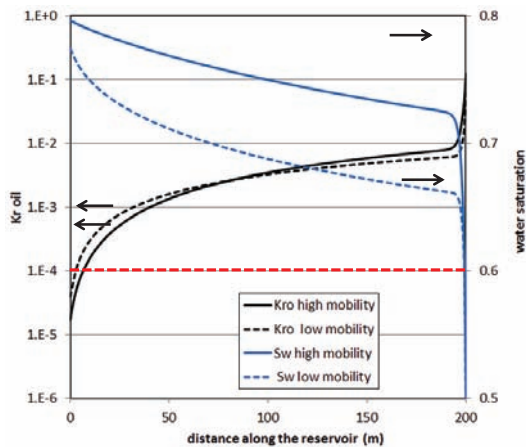


Figure 17 - Numerical simulation for a 1-D reservoir after 30 years of production: water saturation and Kro profiles for 2 values of oil mobility.

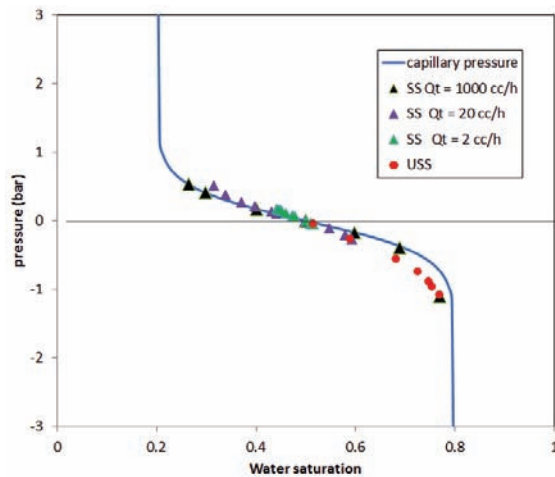


Figure 18 - Range of saturations obtained during the USS and SS displacements performed at various flow rates.

## DISCUSSION

We will first present the advantages and drawbacks of SS and USS methods without focusing on the flow rate. We will then discuss how to deal with the fact that reservoir velocities are much lower than designed front velocity. We will finally discuss the notion of residual oil saturation, laboratory values compared to reservoir final recovery.

### One fluid injected (USS)

The main drawback is that there is no possibility to have saturations in the positive part of the Pc curve and this method cannot be used for water-wet cases. In addition, when the negative Pc presents a flat plateau, it is difficult to adjust the flow rates to have regularly-distributed saturations. This point is the main limitation of the USS multi-rate method.

### Two fluids injected (SS)

Simultaneous injection of oil and water (SS) allows a precise control of saturations. When two fluids are injected at high flow rate, saturation is close to be uniform on a large part of the plug, and its value is mainly controlled by the ratio of viscous forces in the two fluids. This method can be used for any type of wettability. At lower flow rates, the range of saturation is limited (Figure 18).

### How to avoid high flow rates during laboratory experiments?

The first answer is to increase the length of the core. Horizontal cores do not exceed 8-10 cm and the standard solution was to use composite cores, several cores put together in the same coreholder. Now, in-situ saturation monitoring shows that there is a huge discontinuity at each contact (Figure 19), and composite cores should be avoided. A better compromise is to take vertical plugs with length around 20 cm.

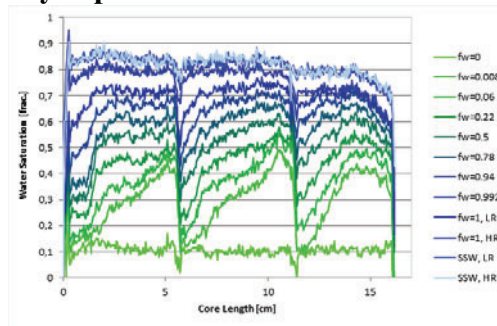


Figure 19 - In-situ saturation monitoring along a composite core showing the discontinuity at each interface.

What is the difference with reservoir? If a 8 cm slice of the reservoir is considered as a plug, the main difference with laboratory is that the condition at outlet is not  $P_c=0$  (this condition is only imposed at the producing well) and local capillary pressures are much higher in the reservoir (see pressure profiles in Figure 16). Semi-permeable porous plates can be used to increase the  $P_c$  inside the sample. However, due to the huge pressure drop through the porous plates and their possible partial invasion, it is not possible to derive directly the  $K_r$  from standard porous plate experiments (Lenormand *et al.* [9]). Brown in 1951 [10] used a modified Hassler core holder with ceramics plates to measure "dynamic capillary pressures" and to compare them to "static" values, but there was no result for relative permeability. Oil was injected and produced through the ceramic plates and gas through grooves at the contact between ceramics and the sample. A similar equipment was patented by Rose in 1985 [11] for  $K_r$  measurement. More recently, Egermann and

Fleury [12] have described an apparatus to measure  $K_r$  behind the porous plates, but their equipment does not allow an outlet boundary condition different from  $P_c = 0$ . Centrifuge experiments could be a solution to allow high capillary pressure with low flow rate. However,  $K_r$  measurements with centrifuge are challenging (Bauget et al. [13]).

### Recommended procedure

We will give an example using our numerical simulations. The lower saturations ( $P_c > 0$ ) can be reached only using the Steady-State method. The range of saturations as function of total flow rate is displayed in Figure 18. The highest flow rate can cover all ranges of saturation but a flow rate of 20 cc/h is preferred in order to approximate reservoir velocities. However, this rate limits the final saturation to 0.6. Afterwards a one-fluid injection (USS) is performed with several steps to estimate the negative part of the  $P_c$  curve, giving information on the wettability.

### Asymptotic values for $S_{or}$

Our last point of discussion concerns the residual oil saturation ( $S_{or}$ ). When using an analytical function for  $K_r$  representation during numerical simulation (Corey or LET), the asymptotic  $S_{or}$  value ( $P_c \rightarrow -\infty$ ) is often equal to zero. For instance, the result presented by Kokkedee (Figure 2) shows a tendency to reach asymptotic zero  $S_{or}$  value. This result is not in contradiction with physical mechanisms: when samples are not strongly water-wet, oil can flow very slowly on the surface of the solid up to very low saturation when pressure is increased. However, this asymptotic value is not the final value reached in reservoir production because capillary pressures are always limited, due to the low mobility of oil, as shown in Figure 16.

## CONCLUSIONS

- One-step experiments, generally referred to as JBN experiments, must be avoided even if they are interpreted with  $P_c$  curves. Their interpretation is based on transient flow dominated by viscous fingering and/or channeling, which does not represent "true" pore-scale relative permeability.
- A more accurate experiment requires 7 to 10 steps: saturations become more uniform after the first step, and flows are then controlled by local  $K_r$ .
- Capillary end effect is not an artifact that should be removed but rather an advantage that allows exploration of all the range of saturations. Conducting  $K_r$  (or EOR) experiments at maximum speed as described in [14] is not a recommended solution. However, with standard displacement experiments, either SS or USS, the balance between capillary and viscous forces requires fluid velocities to be much higher than in reservoirs. An ideal experiment should be able to provide high capillary pressure with low flow rate. Solutions should be investigated using porous plate or centrifuge methods.
- $K_r$  determination during experiments with capillary effects is only possible with numerical simulators. Numerical simulators are also useful to design the experiments.
- When a single fluid is injected (unsteady-state, USS), the range of saturation is controlled by the balance between viscous and capillary forces. Consequently, the experiment is difficult to design if the  $P_c$  curve is not well-known.

- Steady-state method allows a precise control of saturations. When two fluids are injected at high flow rates, saturation is close to be uniform on a large part of the plug, and its value is controlled by the ratio of viscous forces in the two fluids. This method can be used for any type of wettability. At low flow rate, the range of saturation is limited to a small interval around the saturation where  $Pc=0$ .
- Based on these observations, the recommended procedure is a compromise between SS and USS methods.
- We finally show how the Sor measured in laboratory by history matching may defer from the true reservoir Sor.

## ACKNOWLEDGEMENT

We want to thank Jos Maas and Karl Sigurd Årland for providing authorizations to reproduce their figures and Fabrice Bauguet for useful comments on the manuscript.

## REFERENCES

1. Ayub, M. and R.G. Bentsen, "Interfacial viscous coupling: a myth or reality?", (1999), J. Petroleum Science and Engineering, Vol 23.
2. Lackner, A.S., O. Torsaeter, "Phase pressure measurements: simultaneous and direct derivation of relative permeability and dynamic capillary pressure", (2005), SCA2005-05.
3. Johnson, E.F., D.P. Bossler, and V.O. Naumann, "Calculation of Relative Permeability from Displacement Experiments", Transactions AIME, 216, 1959, 370-372.
4. Kokkedee, J.A, W.Boom, A.M. Frens and J.G. Maas, "Improved Special Core Analysis: Scope for a reduced residual oil saturation", (1996), SCA9601.
5. Mohanty, K.K. and A.E. Miller, "Factors influencing unsteady relative permeability of a mixed-wet reservoir", (1988), SPE18292.
6. Fenwick, D., N. Doerler, and R. Lenormand, "The effect of heterogeneity on unsteady-state displacements", (2000), SCA2000-30.
7. Sarma, H.K., B.B. Maini and G. Allen, "Effect of viscous instability on unsteady-state relative permeability", (1992), Revue Institut Français du Pétrole, Vol. 47, Nov-Dec.
8. Lombard J.-M., P. Egermann and R. Lenormand, "Measurement of Capillary Pressure Curves at Reservoir Conditions", (2002), SCA 2002-09.
9. Lenormand R., P. Delaplace and P. Schmitz, "Can we really measure the relative permeabilities using the micropore membrane method", (1996), SCA9637.
10. Brown H. W., "Capillary pressure investigations", Petroleum Transactions, AIME, vol. 192, (1951), also SPE-951067-G.
11. Rose W. D., "Apparatus and procedure for relative permeability measurements", US patent number 4,506,542, 1985.
12. M. Fleury, P. Poulain and P. Egermann, "A new approach to derive relative permeability data while measuring resistivity index, SCA2005-04.
13. F. Bauguet, S. Gautier, R. Lenormand and A. Samouillet, "Gas-liquid relative permeabilities from one-step and multi-step centrifuge experiments", (2012), SCA2012-13.
14. Masalmeh, S.K, "Determination of waterflooding residual oil saturation for mixed to oil-wet carbonate reservoir and its impact on EOR", (2013), SPE-165981-MS.